

SafeWind



Collaborative project funded by the European Commission
under the 7th Framework Program, Theme 2007-2.3.2: Energy

“Multi-scale data assimilation, advanced wind modelling &
forecasting with emphasis to extreme weather situations
for a safe large-scale wind power integration”

Grant Agreement N°: 213740

Deliverable Dp-4.5

“WEATHER PATTERN CLASSIFICATION METHODOLOGY”

DOCUMENT TYPE	Deliverable
DOCUMENT NAME:	swind.deliverable_Dp-4.5.Template_v1.2.pdf
VERSION:	V1.2 ^(*)
DATE:	2010.12.13
CLASSIFICATION:	R0: General Public
STATUS:	Approved/Released

Abstract: This Deliverable of SafeWind project presents the state of the art in wind power forecasting. A number of 824 references of journal and conference papers have been reviewed.

AUTHORS ¹ , REVIEWERS			
MAIN AUTHOR/EDITOR:	F. Valero		
AFFILIATION:	UCM		
ADDRESS:	Facultad de Física. Ciudad Universitaria s/n. 28040 Madrid, Spain.		
TEL.:	+34-91.304.45.20		
EMAIL:	valero@fis.ucm.es		
FURTHER AUTHORS:	M.L. Martin, A. Pascual		
PEER REVIEWERS:	J. Sanz (CENER), P. Chevaux (MeteoFrance)		
REVIEW APPROVAL:	Approved :	<input checked="" type="checkbox"/>	Rejected (improve as indicated below) : <input type="checkbox"/>
SUGGESTED IMPROVEMENTS:	For a long list of remarks make reference to another document		

VERSION HISTORY			
VERSION ² :	DATE:	COMMENTS, CHANGES, STATUS:	PERSON(S):

STATUS, CONFIDENTIALITY, ACCESSIBILITY							
STATUS:			CONFIDENTIALITY:			ACCESSIBILITY:	
S0	Approved/Released	<input checked="" type="checkbox"/>	R0	General public	<input checked="" type="checkbox"/>	Private web site	<input type="checkbox"/>
S1	Reviewed	<input type="checkbox"/>	R1	Restricted to project members	<input type="checkbox"/>	Public web site	<input checked="" type="checkbox"/>
S2	Pending for review	<input type="checkbox"/>	R2	Restricted to European Commission	<input type="checkbox"/>	Paper copy	<input type="checkbox"/>
S3	Draft for comments	<input type="checkbox"/>	R3	Restricted to WP members + PL	<input type="checkbox"/>		<input type="checkbox"/>
S4	Under preparation	<input type="checkbox"/>	R4	Restricted to Task members +WPL+PL	<input type="checkbox"/>		<input type="checkbox"/>

¹ The authors of this document are solely responsible for its content, which does not represent the opinion of the European Community and the European Community is not responsible for any use that might be made of data appearing therein.

² **VERSION NAMING** : V0.x draft before peer-review approval, V1.0 at the approval, V1.x minor revisions, V2.0 major revision

Contents

Chapter 1	4
Chapter 2	8
Chapter 3	18
Chapter 4	46
Chapter 5	56
Chapter 6	74
Appendix I	80
Appendix II	86
References	92

Chapter 1

Introduction

The climatic system presents, as out-standing characteristic, great variability in its behavior, consequence not only of the complex character of the atmospheric dynamics, but also of the existing processes of feedback among the atmosphere and other components of the system, the hydrosphere, the biosphere, the lithosphere and the criosfera (Bonan et to., 1992; Bojariu, 1997; Zeng and Neelin, 2000; Allison et to., 2000; Calov et to, 2003). There are also external factors influencing climate variability, such as solar radiation (Tinsley, 1988). The influence of all these factors may be due to instabilities, resonant modes or nonlinear stochastic processes of not linear nature intrinsic to own climate system components (IPCC The Scientific Basis, 2001).

In the study of the climatic variability it is necessary bear several aspects in mind, such as its origin and the different scales in which it is shown up spatially and temporarily. It is, therefore, necessary to define in a precise way a space and time resolution that allows to rigorously describe the understudy phenomena. Also, it is necessary to select a suitable set of variables that contains the essential information to solve with accuracy the equations that govern the phenomena submitted for consideration (Pedlosky, 1987).

The climatic large-scale characteristics are described, generally, in regular grids that offer a great advantage opposite to the observations on weather stations, since the former cover an area in a regular way. These databases are obtained in several ways, either through interpolation of observational data, or by analyzing forecast from meteorological models applying complex techniques of assimilation of observational data to generate spatially and temporally homogeneous databases.

Large-scale variables reveal recurring patterns called teleconnection patterns that are responsible for the anomalous weather patterns occurring simultaneously in distant places. These teleconnections are reflected in pattern changes of location and intensity of jet streams, wind, temperature, rainfall, storm tracks, etc. The atmospheric circulation, at different atmosphere levels, associated with these patterns, especially at middle latitudes, come to be the origin of much if not most of the variability of different atmospheric fields (Parker et al., 1994, Hurrell 1995, Hurrell and van Loon, 1997; Slonosky, 1999; Slonosky et al., 2001). Although local factors greatly influence the behavior of regional variables, much of the observed variability in their fluctuations is associated with specific patterns of large-scale circulation. Consequently, the characteristics of atmospheric circulation determine much of the variability of regional climate variables (Jacobeit et al., 2003). It is therefore necessary to identify recurrent large-scale patterns to characterize a particular region.

This report deals with the study of atmospheric variability in the Atlantic region and its relationship to the wind field. A weather pattern classification is shown by means of a multivariate methodology. The most predominant variability patterns will be identified considering two windows: one based on the Iberian Peninsula and another one covering most of Europe. Each significant mode will be explained in terms of different teleconnection patterns and/or other atmospheric features. Once the most significant atmospheric patterns are selected and their

relationships with the observational Iberian wind analyzed, a set of dates associated with extreme atmospheric situations will be delivered.

The technique, based on obtaining principal components of different datasets, will be applied in order to extract the most remarkable atmospheric characteristics associated with the two windows.

The delivery is organized as follows: An explanation of the data sets, windows and methodology employed in this delivery is given in Chapter 2. Chapters 3 and 4 are devoted to show descriptions of the results obtained from the applied methodology in both windows. Chapter 5 shows the relationships between observed wind speed and the large-scale atmospheric variables for the Iberian window. Moreover, the methodology will be applied to a European window to study the atmospheric circulation features at a broader scale. Even though wind data are not available at this moment for the Principal Component analysis, some relationships are provided. Additionally, an appendix with statistical explanations of the methodology and the references cited in the delivery are presented.

Chapter 2

Data and Methodology

Atmospheric circulation variability constitutes one of the most important factors in determining spatial distribution changes of variables such as wind, precipitation, temperature and other climatological elements. In southern Europe, the Mediterranean climate constitutes an issue of great concern within the context of regional climate variability and change studies.

In this chapter, large-scale and regional variables for the Iberian and the European windows are described. Furthermore, Principal Component Analysis (PCA) is applied to each variable to obtain a weather pattern classification. Thus, this multivariate methodology is used in order to find the most important patterns of variability in the North Atlantic area. In this chapter, a revision of this methodology is supported. Additionally, if more explanations are needed, an appendix with the statistical details is also provided.

2.1. Description of the data base. Iberian Window

2.1.1. Large scale variables

The large-scale database used in this study consists of daily means of several variables over a grid of $1.2^\circ \times 1.2^\circ$ (lat x lon) resolution for the period 1971-2007. The variables are extracted from the global data base ERA40 from the European Center Medium Weather Forecast (ECMWF) (Uppala et al., 2005). The data base has been seasonally grouped: Winter (DJF), Spring (MAM), Summer (JJA) and Autumn (SON). The selected domain for this study spans the North Atlantic Ocean, the Mediterranean Sea and part of Europe, covering from 20° N to 60° N of latitude and from 51.5° W to 15.5° E of longitude. Thus, 1995 spatial nodes or grid points for 37 years of temporal record are considered (Figure II-1).

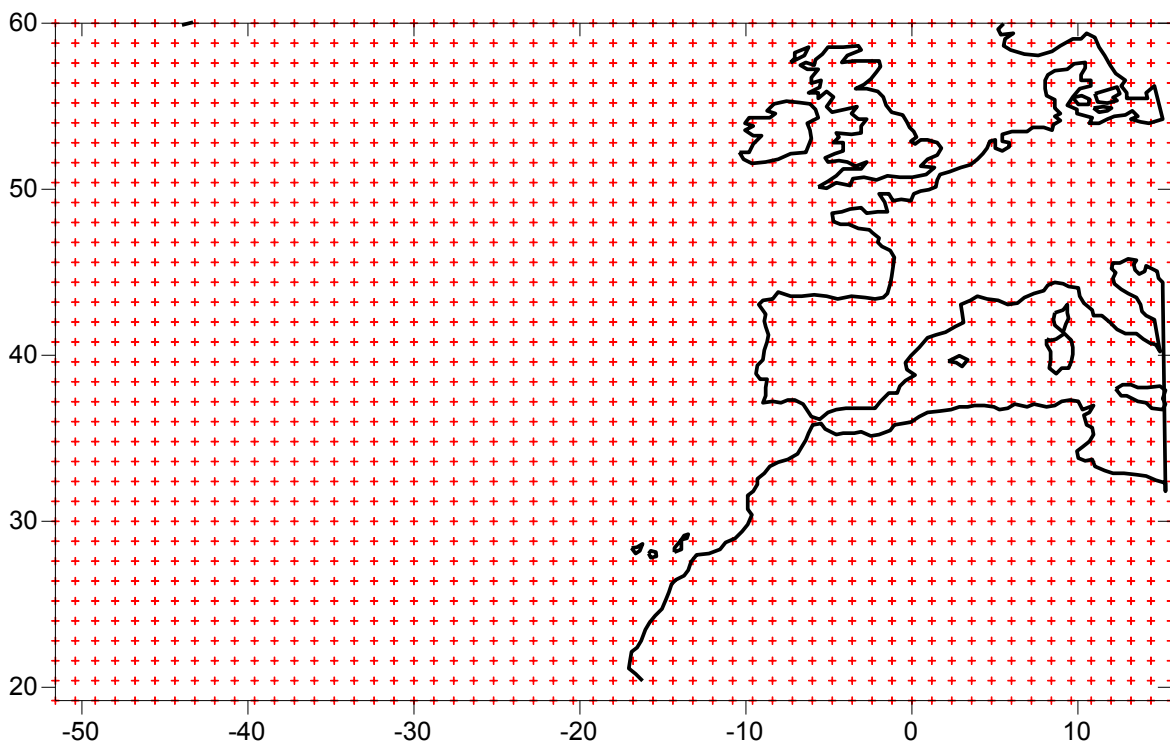


Figure II-1. Geographic coverage of the Iberian window with the spatial nodes at a 1.2° resolution.

The selected large-scale variables are detailed in Table II-1. All these atmospheric variables have been studied in several atmospheric pressure levels. The selected pressure levels have been the following: 1000, 850, 700 and 500 hPa.

VARIABLE	ACRONYM	UNITS
Geopotential height	Z	m^2s^{-2}
Temperature	T	K
Relative humidity	RH	%
Zonal component of wind	U	ms^{-1}
Meridional component of wind	V	ms^{-1}

Table II-1. Large-scale variables, acronyms and units used in the Iberian window.

Prior to the diagnostic analysis all data sets were modified applying a $\cos(\text{latitude})$ square root area-weighting. The reason of this modification is to account for the uneven spatial density of the grid. The original data were also detrended and the seasonal cycle was removed by subtracting the long-term mean to each monthly value. Finally, standardised anomalies were obtained for all fields.

2.1.2. Iberian regional variable.

The main purpose of this delivery is the study of the relationships between the large-scale atmospheric circulation and the wind speed in two different scenarios. One of them is centered on the Iberian Peninsula, analyzing such relationships in terms of availability of observational wind data. The other one will give idea about the origin of the air masses, studying several important atmospheric patterns over Europe. To this end the time period associated with greatest temporal coverage is chosen.

Regarding the regional variable in the Iberian window and in order to obtain mean wind values and a set of statistical scores related to climatic details, the metadata of each station are taken into account. The data come from in-situ measurements of the station network of the Spanish Meteorological Service (Agencia Estatal de Meteorología, AEMET). Over a spatial domain spanning the Iberian Peninsula and the Balearics for a time record covering 1937-2008, observational data such as wind direction, wind velocity, gusts and 6 hourly speed wind data (00, 06, 12 and 18 h) were used. Although 73 stations are initially available in a first study, 25 stations of them had missing data in all variables with

large gaps occurring in large contiguous blocks as it can be observed in the following figure (Figure II-2).

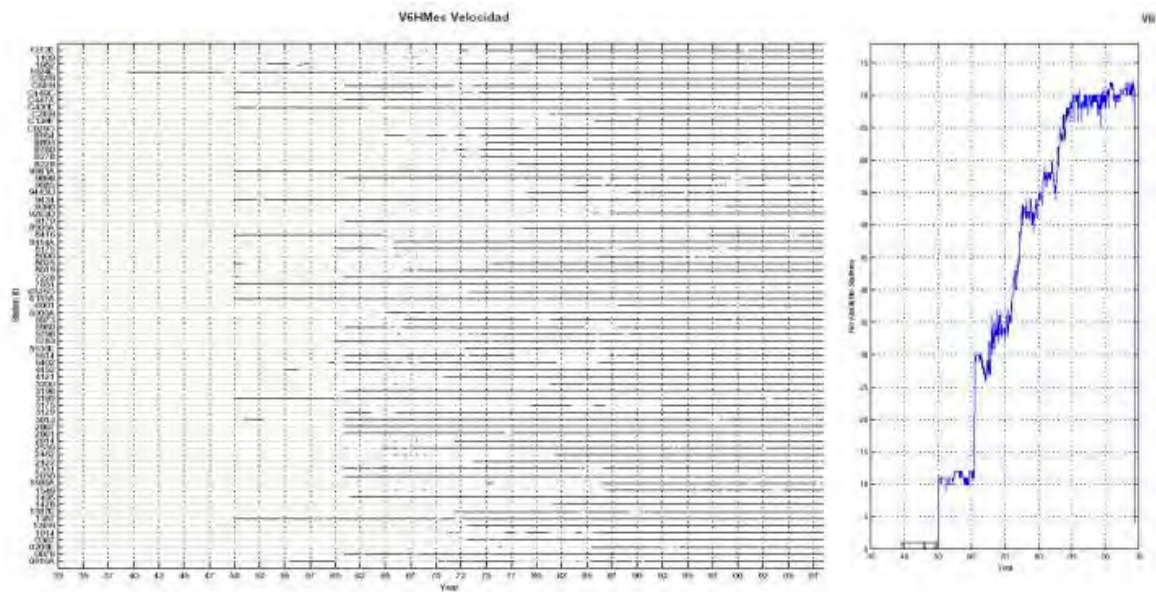


Figure II-2. Left panel: Presence or not presence of data (continuous line) for the stations code versus time period. Right panel: Evolution of number of stations with available data versus time period.

In the left panel of Figure II-2, each line denotes when wind data are available over the time in every station throughout the time period. It can be noticed the existence of large gaps occurring in large contiguous blocks, which make impossible the use of such station. In the right panel, the number of available stations with wind data is represented against the time period. It is noticed that this number is continuously increasing till the 80s decade maintaining the number more or less constant from that date onwards. Finally, those stations with temporal record with at least 15 years of data were considered.

Taken into account these situations, 48 stations are considered with missing data not occurring in large contiguous blocks (station locations will be displayed by dots in the Figure II-4). The time series are analyzed during all time record considering in total a time record from 1980 to 2001 (Figure II-3).

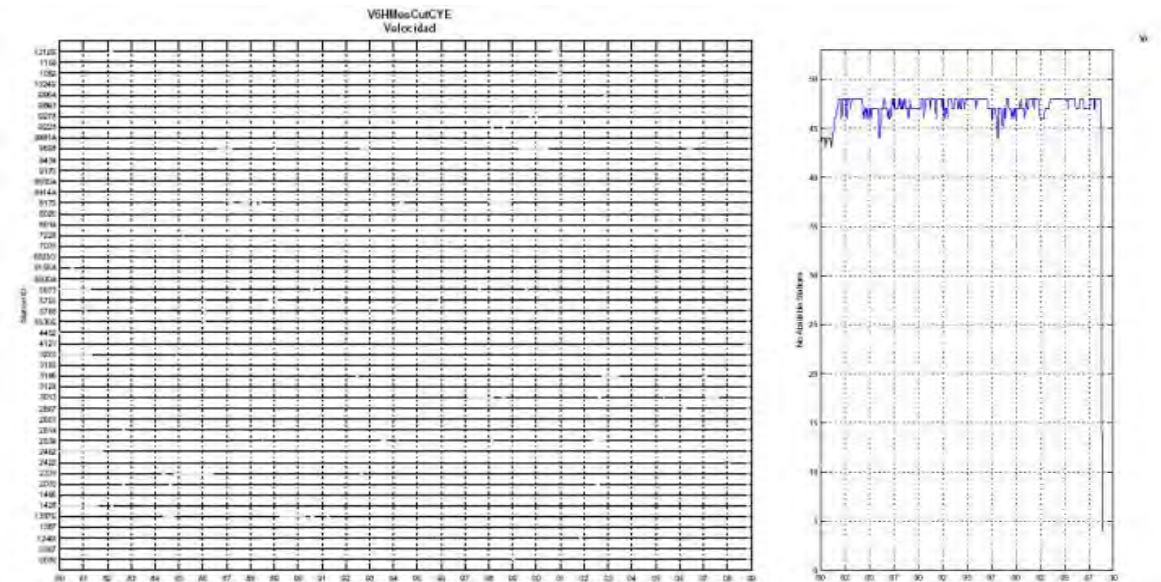


Figure II-3. Left panel: Presence or not presence of data (continuous line) for the stations code versus time period. Right panel: Evolution of the final number of stations with available data versus time period.

All wind variables were analyzed taken into account the missing data, **manipulation errors, trends, inhomogeneities,** Then, the 6-hour wind speed data were selected. In such quality control process, several stations were removed from the database for further analyses. Thus, from the 6-h wind data, time series of daily and monthly mean wind speed were built for those 23 stations (Table II-2), passing the quality control process (station locations are shown in the Figure II-4) and covering the 1980-2001 period. Moreover, a monthly mean wind speed field has been obtained over the 22-year period from the daily data.

The seasonality of atmospheric circulation, reflected by the synoptic scale variability, affects the wind field. Thus, in a first study, the daily and the monthly 6-hour mean wind speed data were seasonally obtained: Winter (DJF), Spring (MAM), Summer (JJA) and Autumn (SON). After applying the approaches to all the data fields finally selected, only the results for winter and for daily data will be provided in order to avoid excessive length of the delivery.

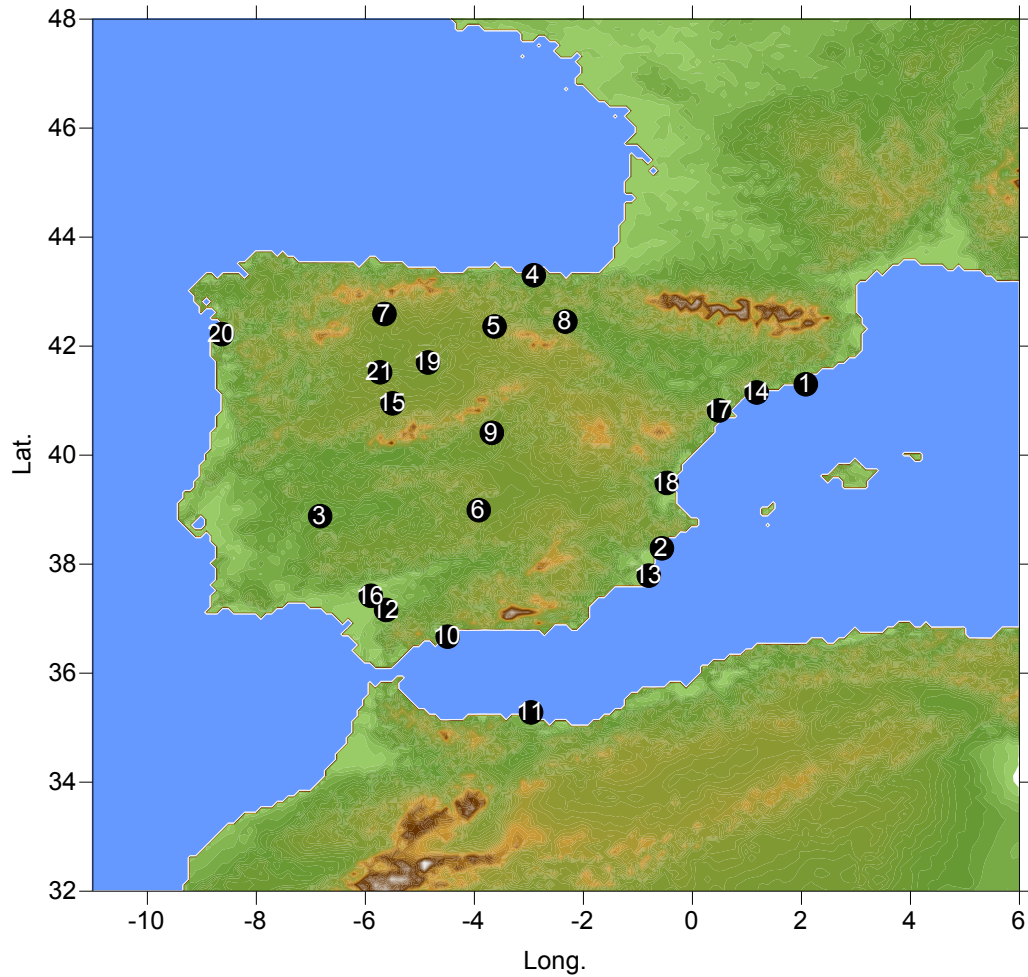


Figure II-4. Numbers indicate the wind stations for the Iberian Peninsula with its orography detailed. The station codes are shown in Table II-2. The x-axis corresponds to longitude, positive (negative) for East (West).

The list of stations used and their geographical coordinates are shown in Table II-2. In analogous way to the large-scale variables described in the previous section, the original data were detrended and the seasonal cycle was removed by subtracting the long-term mean to each monthly value. Finally, standardized anomalies were obtained for all fields. This dataset was quality controlled and homogeneity tested therein.

ID	Name	Lat.	Long.	Elev.
1	AEROPORT DE BARCELONA (EL PRAT)	41.30	2.08	6
2	ALICANTE (AEROPUERTO EL ALTET)	38.29	-0.56	31
2	ALICANTE (CIUDAD JARDIN)	38.37	-0.49	82
3	BADAJOS (TALAVERA 'BASE AEREA')	38.88	-6.83	185
4	BILBAO (AEROPUERTO)	43.30	-2.91	39
5	BURGOS (VILLAFRIA)	42.36	-3.63	890
6	CIUDAD REAL (ESCUELA DE MAGISTERIO)	38.99	-3.92	627
7	LEON (VIRGEN DEL CAMINO)	42.59	-5.65	916
8	LOGROÑO (AGONCILLO)	42.45	-2.33	352
9	MADRID (CUATRO VIENTOS 'AERODROMO')	40.38	-3.79	687
9	MADRID RETIRO	40.41	-3.68	667
10	MALAGA (AEROPUERTO)	36.67	-4.49	7
11	MELILLA	35.28	-2.96	55
12	MORON DE LA FRONTERA (BASE AEREA)	37.16	-5.62	87
13	MURCIA (SAN JAVIER)	37.79	-0.80	2
14	REUS (AEROPORT)	41.15	1.18	68
15	SALAMANCA (MATACAN)	40.95	-5.50	790
16	SEVILLA (AEROPUERTO)	37.42	-5.90	26
17	TORTOSA (OBSER. DEL EBRO)	40.82	0.49	48
18	VALENCIA (AEROPUERTO MANISES)	39.49	-0.47	57
19	VALLADOLID (VILLANUBLA)	41.70	-4.85	846
20	VIGO (PEINADOR)	42.22	-8.63	255
21	ZAMORA (OBSERVATORIO)	41.52	-5.73	656

Table II-2. Large: List of stations used indicating the code for Figure II-4, name, longitude, latitude and altitude.

2.2. Description of the database. European Window

The Principal Component methodology is applied to a European window in order to cover all the Safewind test cases. In this section, only the large-scale atmospheric variables are described. The large-scale data base used in this study consists of daily means data over a grid of $2.5^{\circ} \times 2.5^{\circ}$ (lat x lon) resolution for the period 1958-2007, selected from the global data base ERA40 from European Center Medium Weather Forecast (ECMWF) (Uppala et al., 2005). The data bases have been seasonally grouped: Winter (DJF), Spring (MAM), Summer (JJA) and Autumn (SON). The selected domain for this study spans the North Atlantic Ocean, the Mediterranean Sea and Europe from 20° N to 85° N latitude and from 60° W to 50° E longitude. Thus, 1269 spatial nodes or grid points for 50 years of temporal record are taken into account (Figure II-5).

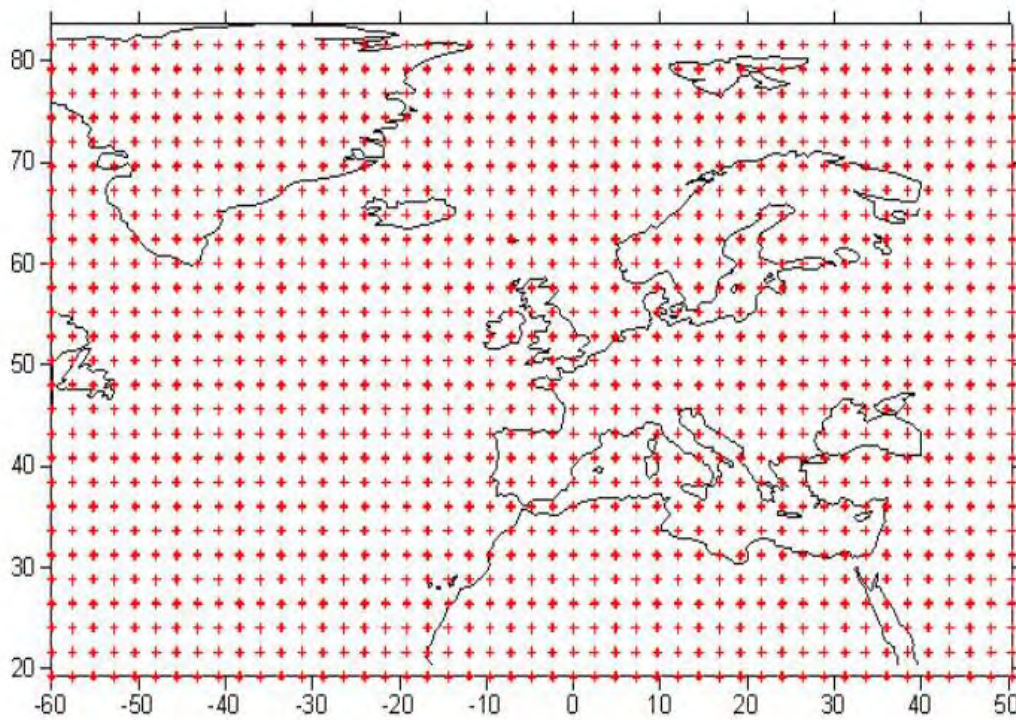


Figure II-5. Geographic domain of the European window with the spatial nodes at a 2.5 resolution.

The selected large-scale variables are detailed in Table II-3. They are studied at 1000, 850, 700 and 500 hPa pressure levels.

VARIABLE	ACRONYM	UNITS
Mean sea level pressure	SLP	Pa
Geopotential height	Z	m^2s^{-2}
Temperature	T	K
Relative humidity	RH	%
Zonal component of wind	U	ms^{-1}
Meridional component of wind	V	ms^{-1}

Table II-3. Large-scale variables, acronyms and units used in the European window.

As in the Iberian window case, prior to the diagnostic analysis all data sets were modified applying a $\cos(\text{latitude})$ square root area-weighting to account for the uneven spatial density of the grid. The original data were also detrended and the

seasonal cycle was removed by subtracting the long-term mean to each monthly value. Finally, standardised anomalies were obtained for all fields.

2.3. Methodology: Principal Component Analysis.

In order to extract the spatial and temporal behaviour of a data set, principal component analysis (PCA) has been applied to the large-scale atmospheric circulation and the wind databases in the case of the Iberian window. For the European window it is only applied to the large-scale variables.

The PCA has proven to be a reliable method for data reduction and for examining the variance structure (Preisendorfer 1988). The following sketch summarizes the PCA procedure. The methodology, applied to spatial data, \mathbf{X} , known as S-mode decomposition (Richman 1988), enables patterns to be identified that can be attributed to specific physical processes by statistical assessment. The new uncorrelated variables are called principal components (PCs, a_{ij}) and consist on linear combinations of the original variables derived from the diagonalisation of the covariance/correlation matrix \mathbf{R} . The coefficients of the linear combinations P_{kj} represent the weight of the original variables in the PCs and they are named *loadings* or PC patterns. The PCs indicate modes of variation of the original field and are numbered according with their related variance. Thus, the first PC is the linear combination with the maximum possible variance, the second one is the linear combination with the maximum possible variance which is uncorrelated with the first PC and so on (Jolliffe, 1986; Sneyers et al. 1989) . The projection of the original series onto each eigenvector gives as result the time-dependence coefficient named *scores* or PC time series, a_{ij} .

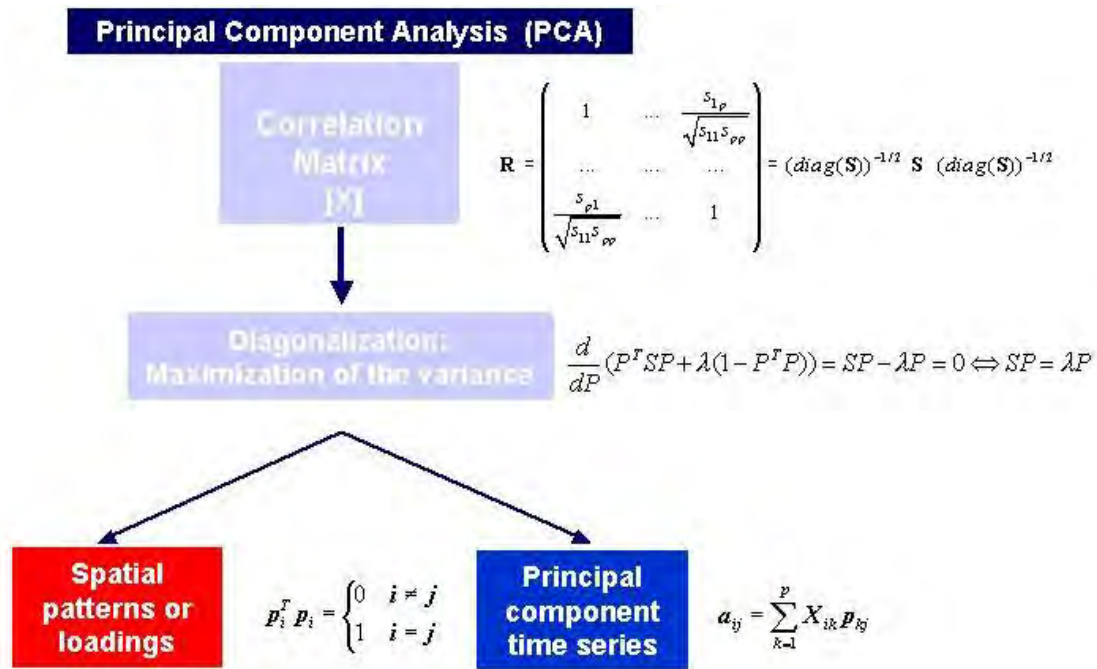


Figure II-6. Sketch of Principal Component Analysis. See Annex I for more detailed information about the methodology.

In our cases, the PCA was applied to the correlation matrices of all datasets, the large-scale variables and observational wind fields, and a set of eigenvalues and eigenvectors were produced. Generally, the most important (the first ones) eigenvectors tend to describe regions with largest fluctuations. Thus, most information from the data can be represented using some smaller number of the principal components and a much smaller data set. The PCA was described by Pearson and Hotelling and it was introduced in meteorology by Lorenz (Lorenz, 1956). For more explanations, more details about the PCA technique are given in Appendix I.

Chapter 3

Results of Principal Component Analysis. Daily data. Iberian window.

The results to be shown correspond to the PCA methodology applied to daily large-scale fields and observational wind speed for the Iberian window. A weather pattern classification is shown by means of the multivariate methodology, also explaining each significant mode in terms of different teleconnection patterns and/or other atmospheric features. The data base is seasonally grouped as it is already mentioned in the previous chapter. Additionally, the results of the PCA of the large-scale datasets corresponding to the European window will be also shown in the following chapter.

Prior the spatial statistical results, tables with variance percentages explained for the most significant PCs or modes for the different large-scale fields, described in the previous chapter, at the 1000 hPa level are shown. Although the PCA has been applied to large-scale fields of several variables at different atmospheric levels, this delivery will be focus on the near-surface geopotential heights for representing the large-scale atmospheric circulation at a more realistic height level for the observational wind speed field over Iberia. In addition, eigenvectors

resulted from the applied PC methodology are also shown as well as their links with the most relevant Atlantic atmospheric patterns. Thus, and for reasons of brevity, explanations will be made only for Z1000 and for winter in the section 3.1 and for spring and Z1000 in the section 3.2. In analogous way, seasonally results of daily regional variable will be also shown.

On the other hand and in order to get information about all timescales involved in the time series derived throughout the study, a wavelet transform analysis has been carried out over all time series obtained. The wavelet transform technique was introduced and formulated by Morlet et al. (1982) and Grossman and Morlet (1984). Wavelet transforms have been applied successfully to different studies of meteorological and climatological time series so as to understand their temporal scales of variability (Gamage and Blumen, 1993; Gao and Li, 1993; Weng and Lau, 1994; Morata et al., 2006; Barbosa et al., 2009). These studies highlight the advantages of the technique compared to Fourier transform analysis since wavelets can show structures both in the spatial and time domains. The Fourier transform does not contain any time dependence on the signal, hence not providing any local information regarding the time evolution of its spectra. One of the differences with the Fourier transform is that wavelets enable localization in frequency and in time (Morlet et al., 1982), turning to be an appropriate and powerful tool to study time series.

3.1. PCA results of large-scale variables. Meteorological analysis of the first modes in winter. Iberian window

The following table displays the variance percentages accounted for the most significant PCs or modes for the large-scale fields, geopotential height, temperature and relative humidity, at the 1000 hPa level.

Level(hPa)	Component	Z(var)	T(var)	HR(var)
1000	1	25.25	14.14	5.47
	2	20.07	12.69	5.27
	3	14.01	8.56	4.91
	4	9.21	7.68	4.25
	5	7.34	5.78	3.63
	6	4.38	5.07	3.27
	7	3.52	3.83	2.51
	8	2.82	3.64	2.26
	9	1.94	3.33	2.19
	10	1.54	2.61	2.03

Table 3.1. Variance percentages of the first ten PCs for geopotential height, temperature and relative humidity at 1000 hPa level.

The Figure III-1-2-3 shows eigenvectors or spatial patterns associated with the ten first PCs, the most significant modes, obtained from the application of the PCA to the geopotential height, temperature and relative humidity.

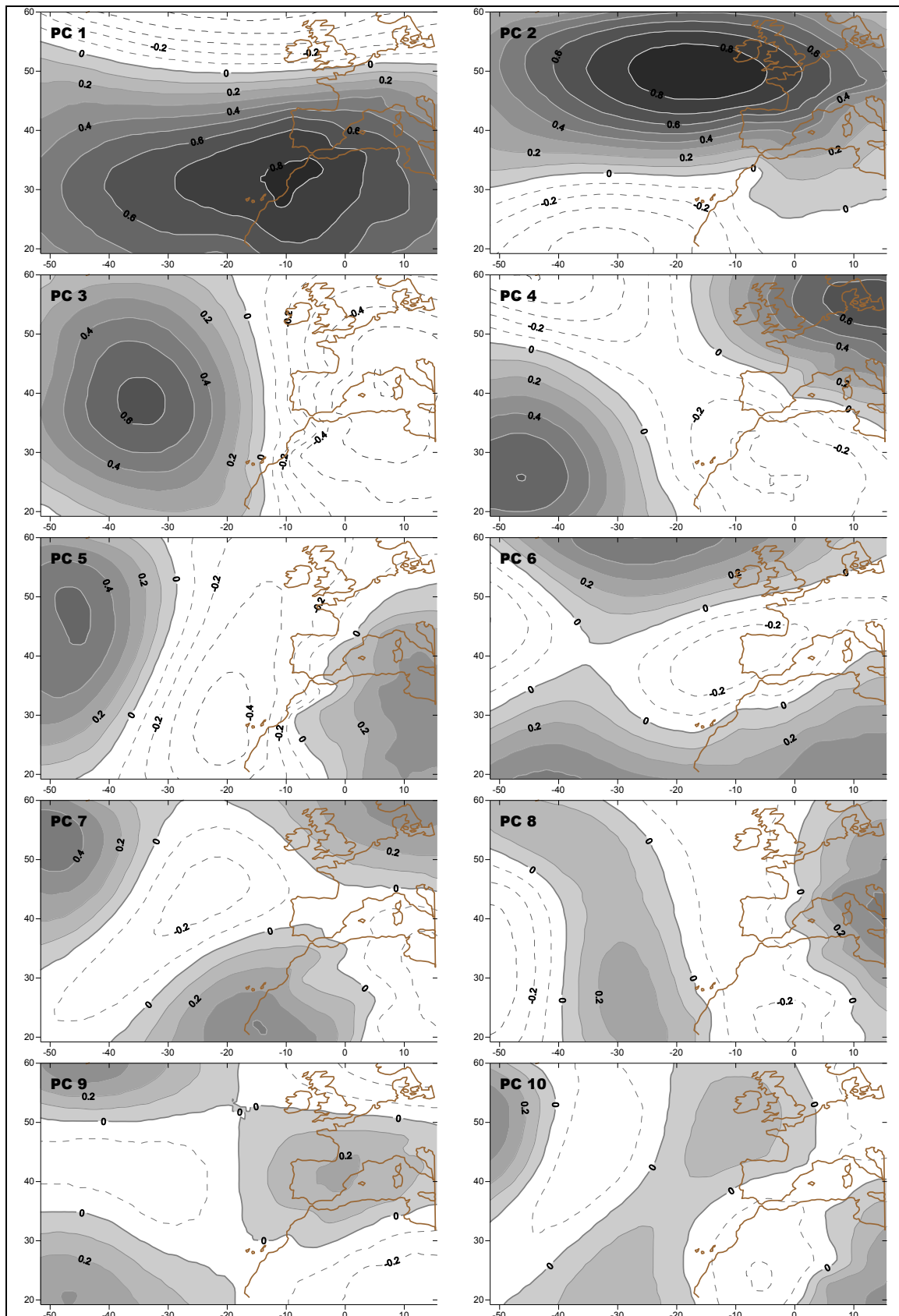


Figure III-1. The first ten PCA patterns of geopotential height at 1000 hPa for winter. Contours indicate correlation values.

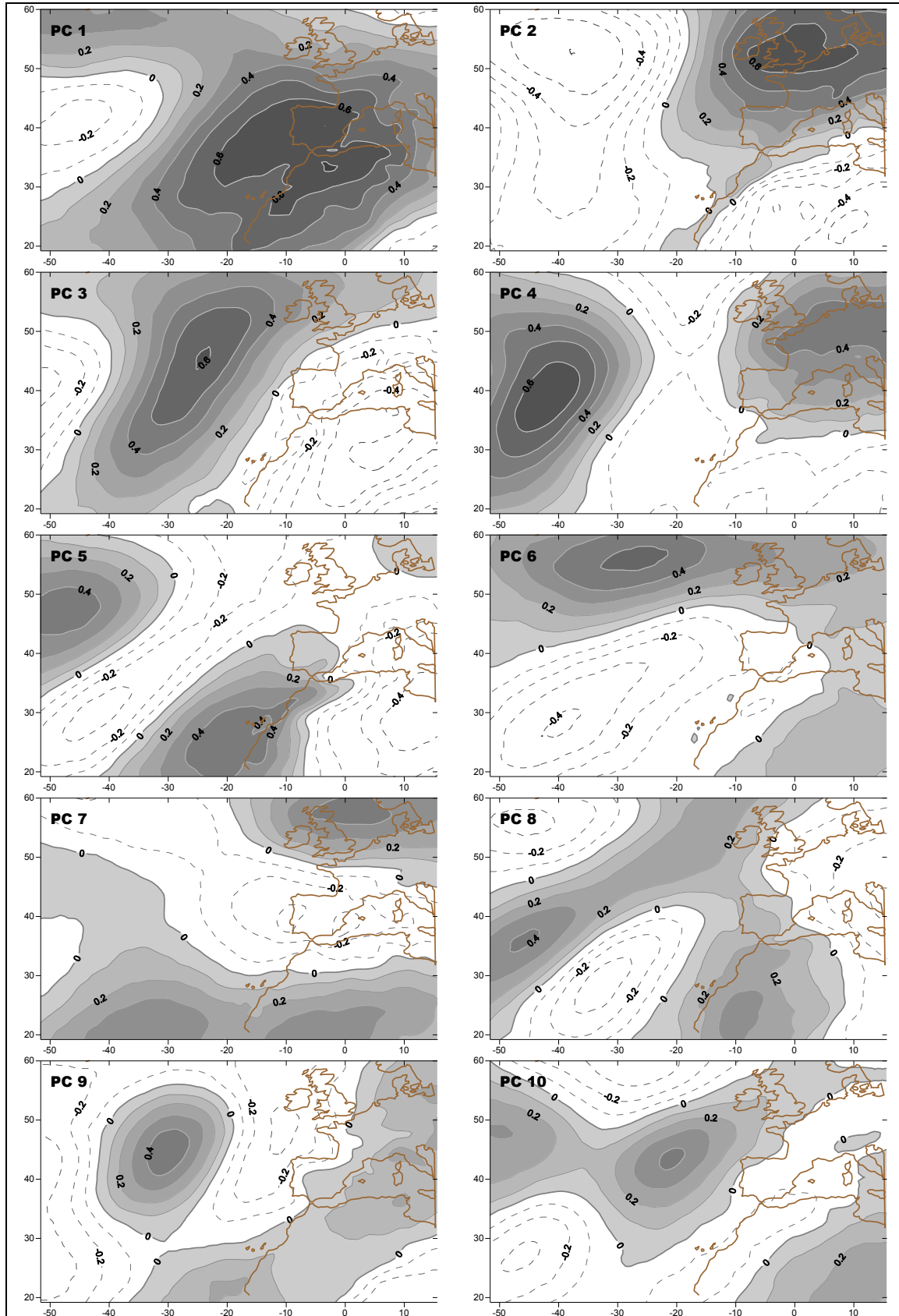


Figure III-2. The first ten PCA patterns of temperature at 1000 hPa for winter. Contours indicate correlation values.

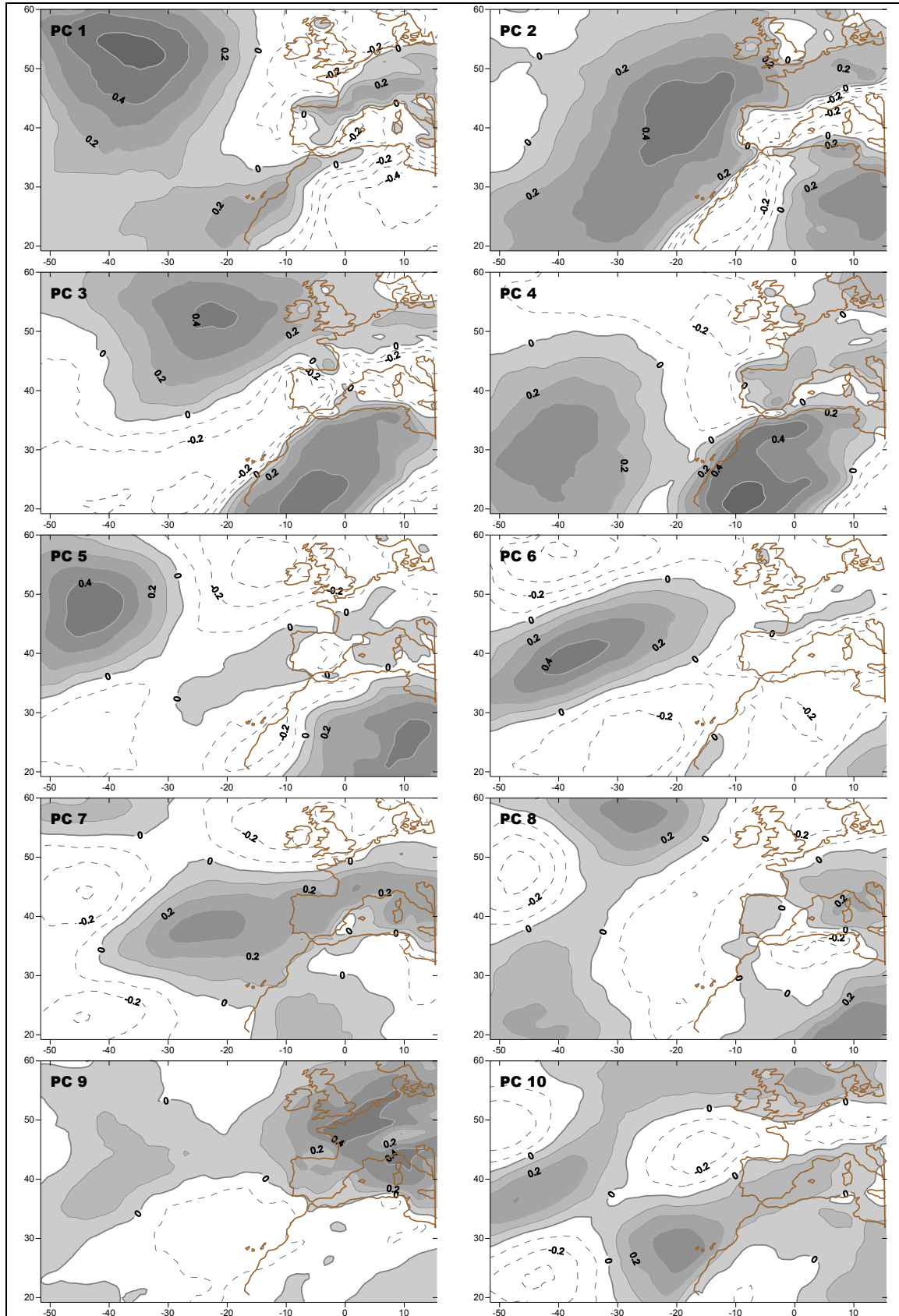


Figure III-3. The first ten PCA patterns of relative humidity at 1000 hPa for winter. Contours indicate correlation values.

In this section the first ten significant modes obtained from the PCA are illustrated in terms of their spatial configurations and their temporal evolutions, describing how the spatial configurations are representative of several Atlantic teleconnection patterns.

First mode

The first mode obtained from the application of the PCA accounts for the main percentage of variance of the original data. Thus, this obtained PC represents the most representative mode. It is noticed high correlation values in the first mode of the three analyzed variables (Figuras III-1, III-2 and III-3), being arbitrary the sign of the isolines. The Z1000 geopotential pattern (Figure III-1) is characterised by a north-south dipole configuration. One of the two centres is located centred over the Canary Islands while the other one is situated eastward Greenland. The spatial pattern shows a meridionally gradient similar to the well known North Atlantic Oscillation, NAO, teleconnection pattern (Barnston and Livezey, 1987). This pattern is characterized by below normal pressure across the high latitudes and above normal pressure over the central North Atlantic Ocean, the eastern United States and Western Europe (Barnston and Livezey, 1987).

The intensification of high pressure over the 35°N promotes extreme westerly wind across the North Atlantic Ocean, below normal temperatures in western Greenland and above normal temperatures over the eastern area of the United States and northern Europe (Figure III-2). Additionally positive anomalies of precipitation are observed in northern Europe and Scandinavian areas while negative anomalies are located in the southern and central part of Europe (van Loon and Rogers, 1978; Rogers and van Loon, 1979). On the other hand, the intensification of the Iceland low promotes strong southwestern advection favouring maritime air over the European continent.

The time variability of the patterns described by the first significant mode is similar in the three analyzed fields (Z1000, T1000 and HR1000) and is characterized by a marked interannual character. The frequency of positive anomaly episodes is analogous to the frequency of the negative ones. In Figure

III-4, it can be observed the time evolution of the most significant scores or PC time series associated with the Z1000 field. In order to look into the time series, wavelet transforms have been applied to the PC time series. The wavelet transformation has not only good local properties in time and frequency domain, but it also works as a microscopic analytical function by decomposing a time series into a set of scale components. Like Fourier sines and cosines, wavelets are basis functions that can be used to represent any given signal as they contain information about frequencies of the signal over all times instead of showing the frequency variations in time. Wavelet transforms are built as translations and dilations of a mother wavelet, or wavelet function, and of a scaling function. Wavelets are characterized by pairs of the mother orthogonal functions interpreted as impulse response to bandpass filter, and scaling functions that can be interpreted as impulse response to low-pass filter (Mallat, 1998; Kaiser, 1995). Furthermore it allows discrimination between oscillations occurring at fast scales and others at slow scales (Morlet et al., 1982; Grossman and Morlet, 1984; Morata et al., 2006; Morata et al., 2008). Additionally, the continuous wavelet analysis has the advantage of being usually easier to interpret because all the information tends to be more visible. In this study, the continuous wavelet transform was used as a filter to decompose and isolate characteristics (Mallat, 1998) of the time series at different frequencies.

The Figure III-5 displays the wavelet power spectrum displayed as a function of period and time, corresponding to the first PC Z1000 time series. The magnitude of wavelet coefficients gives a measure of the correlation between the signal and the wavelet basis. The power spectrum is mainly characterized by scales evolving between 2 and 8 years (see y-axis of Figure III-5), throughout the whole time period (1971 to 2007), showing power spectrum intensity mainly concentrated in periods between 5 and 7 years. Also it is noticeable an evolution of maximum/minimum nucleus between 1975 and 2001, presenting a period with maximum amplitude around 6 years. There are energetic oscillations in scales below 2 years, indicating intra-year and inter-year variability, also present in the time series evolution of the first PC in Figure III-4. Additionally, periodograms of the time series were derived (not shown) to reveal that the maximum power of

the spectra is concentrated in periods of less than 8 years, showing similarity with the wavelet results shown.

Second mode

The obtained patterns associated with the second mode of the Z1000, T1000 and HR1000 account for the second quantity of variance of the original data. In analogous way of the first mode, it can be observed high correlation values in the three large-scale fields (Figures III-1, III-2 and III-3). The Z1000 pattern shows strong resemblance with the Euro Asiatic teleconnection pattern (EU1) identified by Barnston and Livezey (1987) for geopotential height at Z500 hPa. The EU1 is characterized by a principal circulation node extended over the Scandinavian Peninsula and most of the Arctic Ocean and northern Siberia with two additional nuclei of opposite sign over the southern Europe and the western China (Barnston and Livezey, 1987). The Z1000 pattern obtained from the PCA methodology in the Iberian window presents strong dipolar structure with a centre of high positive anomalies over the North Atlantic Ocean and its negative counterpart located over the southern area of study.

The second mode associated with the T1000 variable presents strong dipolar structure with strong positive anomalies west to the corresponding one of the first mode and another nucleus of negative anomalies over western Europe, directly affecting the Iberian Peninsula (Figure III-2). On the other hand, the HR1000 configuration shows an above normal nucleus over Iberia (Figure III-3). The phase positive and negative periods obtained in the time series of scores result analogous to the observed ones for the EU1 pattern (not shown).

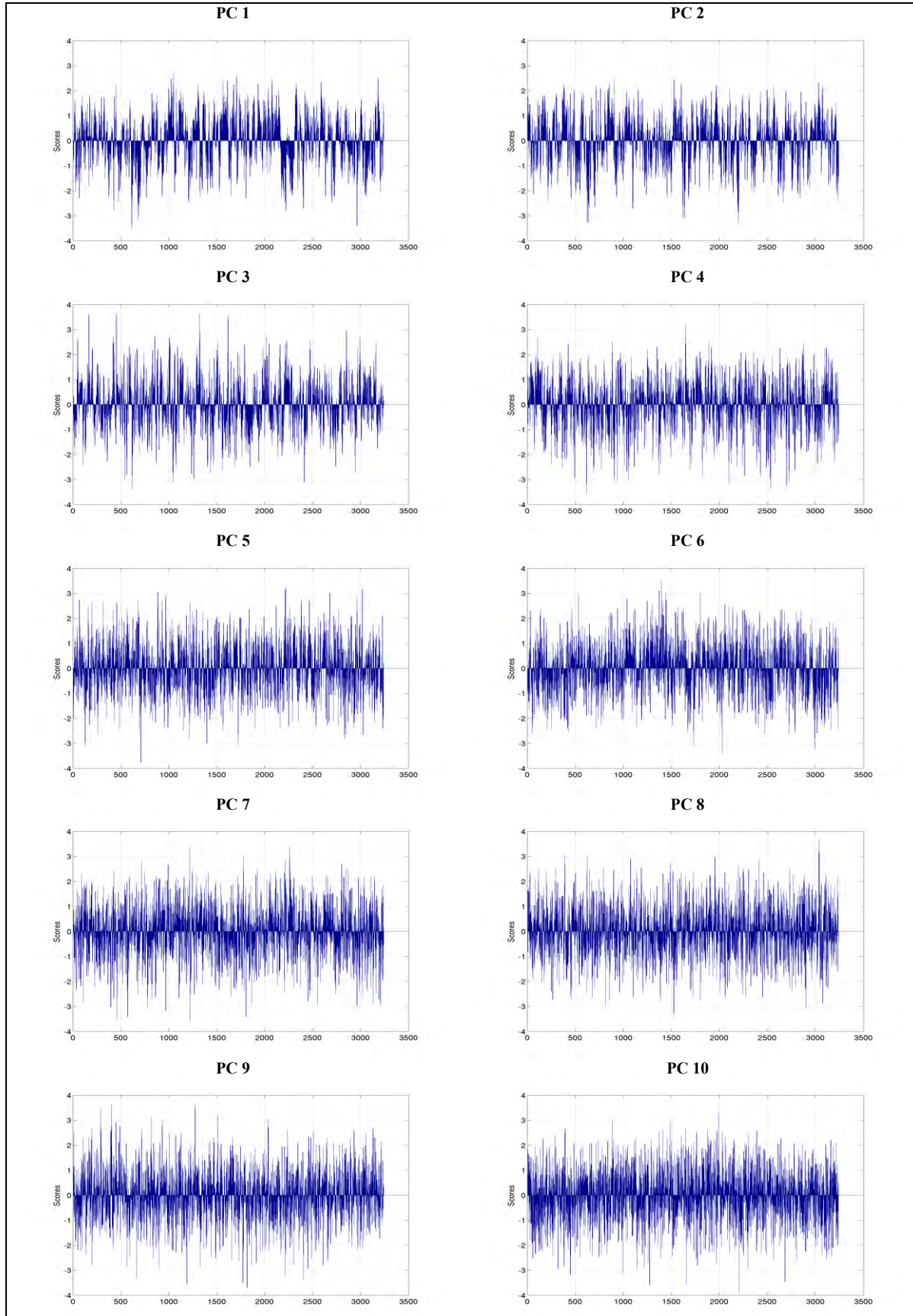


Figure III-4: Time series of PCs corresponding with the first ten modes of Z1000.

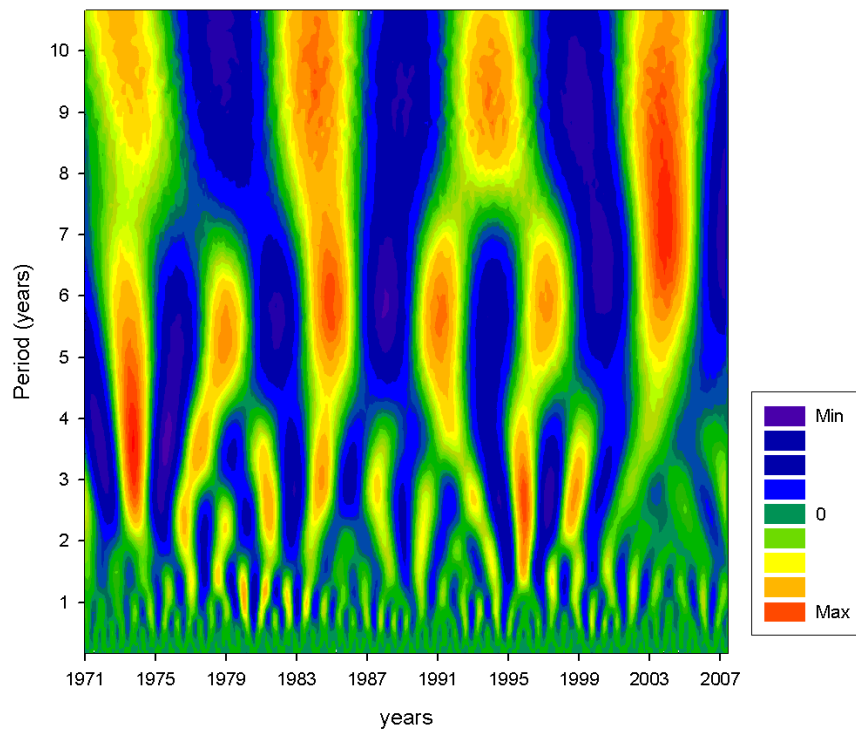


Figure III-5: The wavelet power spectrum of the Z1000 time series corresponding to the first PC. The y-axis represents the variability scale (years) and the x-axis corresponds to the time period.

Third mode

The third most significant pattern obtained for the Z1000 field (Figure III-1) consists of a configuration of positive (negative) correlation values centred over the North Atlantic area (western Europe). Maxima of latitudinal western wind mainly affect northern Europe, Russia and the Scandinavian Peninsula. Meridional flows are maxima in the western North Atlantic area over Iceland producing northern flows over the eastern coast of the United States and in the vicinity of Iberia. Thus, such configuration is dynamically coherent characterized by intrusions of cold air masses over Iberia as it can be noticed in the strong temperature gradient in Figure III-2.

Fourth mode

The fourth mode obtained from the PCA shows a col (Bluestein, 1992) over the Iberian Peninsula. The col (common in the "horse latitudes") is the intersecting zone between an anticyclonic axis (joining two high pressure centres facing each other) and a cyclonic axis (joining two low pressure centres facing each other). A

col is characterised by substantial deformation in their vicinity and consequently is highly related to vorticity and instability. Valero et al. (1997) have shown that these large-scale physical and dynamical configurations are related to extreme rainfall episodes in the Western Mediterranean. Such atmospheric configuration promotes northern (southern) air advection over the northern (southern) Iberia. When over the area there is a cold air mass at upper atmospheric levels, the instability is very high, producing high precipitation and low temperatures.

Fifth mode

This mode presents a spatial pattern very similar to the third mode except for the centre of negative anomalies locate in between two strong nuclei of positive anomalies (Figure III-1). The isolines are longitudinally extended which represents strong northern (southern) air advection over Iberia (remember that the sign of the isolines in the pattern is arbitrary). This situation could be associated with a omega blocking situation (Bluestein, 1992). In the region of the block, the weather remains essentially unchanged, as any transient weather disturbances are forced to circumvent the block. Once established, major blocking situations tend to persist for at least a week and appear to represent some quasi-equilibrium state of the atmosphere.

Sixth mode

The sixth mode is structurally similar to the fourth mode, i.e., it corresponds to a col. The difference between the two modes is in the displacement of the axis (Bluestein, 1992). The axes of the sixth mode (Figure III-1) show a north-south line, associated with the positive correlation centres and negative correlation centres from a west-east distribution. Iberia, under the effect of a negative correlation centre, indicates lower geopotential values than the mean.

Seventh mode

This Z1000 mode shows a pattern similar to the fourth and sixth modes. The isolines correlation configuration (Figure III-1) is weaker than the other modes, leaving the Iberian Peninsular centred on a col. If, at upper levels, cold air masses

are juxtaposed over the col, instability on surface over such area is very intense, leading to strong precipitation and decreased temperature.

Eight mode

The eight mode (Figure III-1) shows over Iberia low negative correlation values in between two zones of positive correlations. This configuration promotes meridionally air mass advection over Iberia with decreasing or increasing temperatures depending on the air direction.

Ninth mode

This mode (Figure III-1) shows a positive correlation centre over Iberia with weaker negative correlation centres around it. The corresponding T1000 (Figure III-2) and HR1000 (Figure III-3) modes show positive correlation nuclei covering the Iberian Peninsula.

Tenth mode

The last significant mode of Z1000 (Figure III-1) presents an omega configuration with a positive correlation centre over eastern Atlantic Ocean flanked by two weaker negative correlation centres. Such isolines configuration promotes northeast advection of air masses over north Iberia and southeast advection over south Iberia with subsequent increase of temperature and humidity (Figure III-2 and Figure III-3).

3.2. PCA results of large-scale variables. Meteorological analysis of the first modes in spring. Iberian window

Following the same methodology as in the previous section, for the data base of geopotential height at 1000 hPa level in springtime, the five most significant PCs or modes account for more than 80% of variance.

The Figure III-6 shows eigenvectors or spatial patterns associated with the five first PCs, the most significant modes, obtained from the application of the PCA to the geopotential height in springtime. In this section the first five significant modes obtained from the PCA are illustrated in terms of their spatial configurations and their temporal evolutions, describing how the spatial configurations are representative of several Atlantic teleconnection patterns.

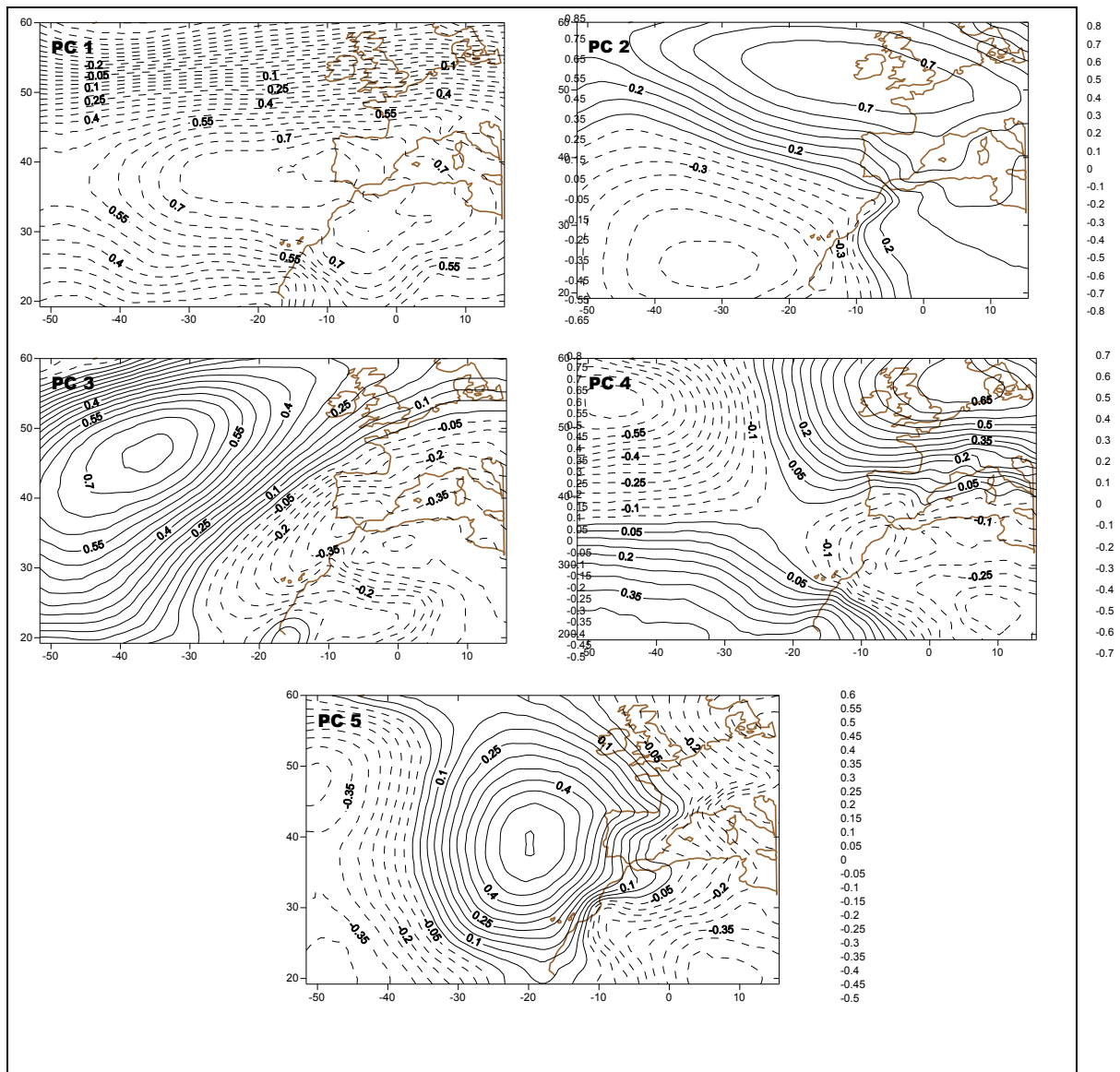


Figure III-6. The first five PCA patterns of geopotential height at 1000 hPa for spring. Contours indicate correlation values.

The first mode obtained from the application of the PCA accounts for the main percentage of variance of the original data (28%), being this obtained PC

represents the most representative mode. The Z1000 geopotential pattern (Figure III-6) is characterised by a strong nucleus centred over the Iberian Peninsula.

The time variability of the patterns described by the first significant modes is, in analogous way than the winter case, characterized by a marked interannual character. In Figure III-7, it can be observed the time evolution of the most significant scores or PC time series associated with the Z1000 field.

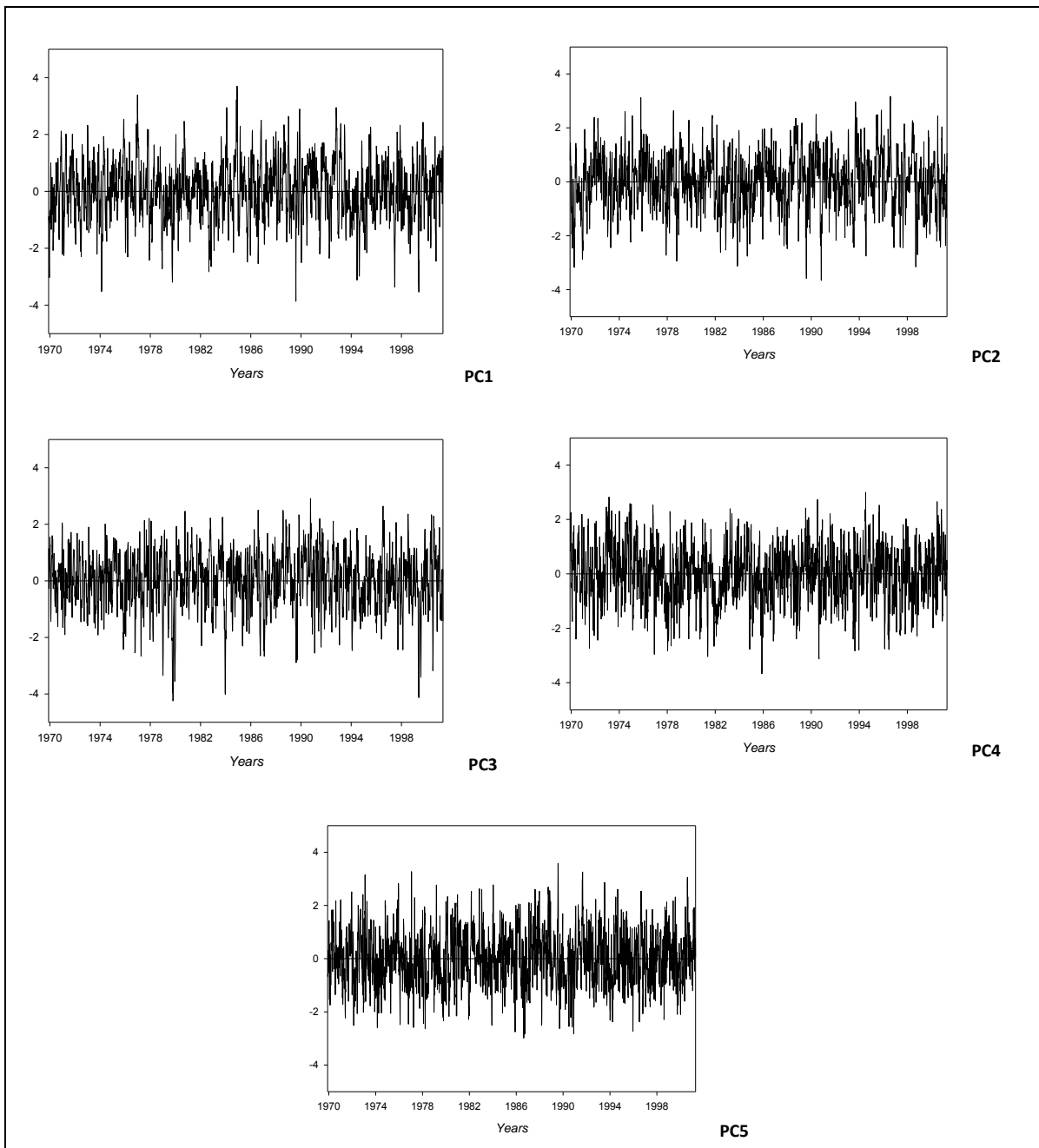


Figure III-7: Time series of PCs corresponding with the first five modes of Z1000 in springtime.

Wavelet transforms have been also applied to these PC time series, showing the power spectrum mainly characterized by scales evolving between 2 and 7 years (see y-axis of Figure III-8), throughout the whole time period (1971 to 2007), showing power spectrum intensity mainly concentrated around the 5-year period. There are some energetic oscillations in scales below 2 years, indicating intra-year and inter-year variability, also present in the time series evolution of the first PC in Figure III-7.

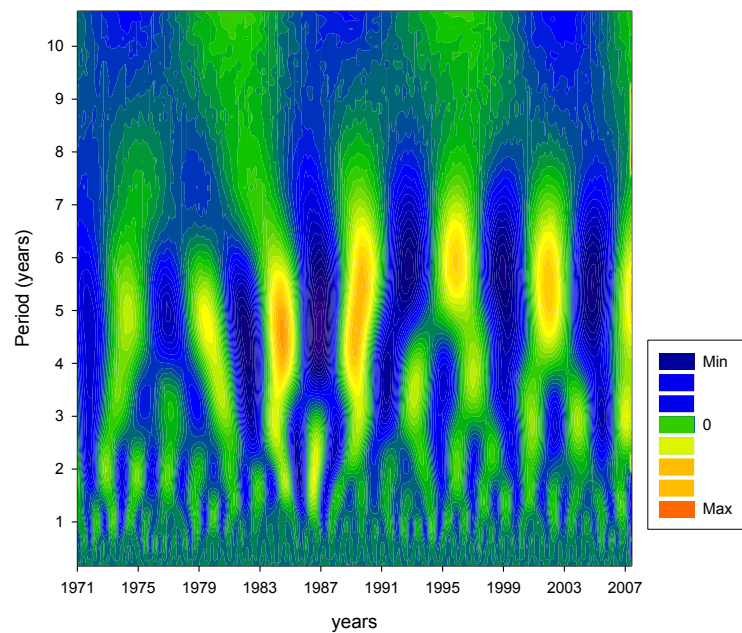


Figure III-8: The wavelet power spectrum of the wind speed time series corresponding to the first PC of Z1000 in springtime. The y-axis represents the variability scale (years) and the x-axis corresponds to the time period.

For the remainder modes, the percentage of variance diminishes, accounting finally for 80% of the total variance. The second Z1000 spatial pattern for the springtime accounts for 24% of variance of the original data. The pattern shows (Figure III-6) two nuclei of strong correlation values, one of them located over the Britain Islands and the other one situated southwestern Canary Islands. The third most significant pattern obtained for the spring Z1000 field (Figure III-6) consists of a configuration of positive (negative) correlation values centred over the North Atlantic area (Western Europe). It is a spatial pattern very similar to the corresponding third mode of the wintertime.

In an analogous way than the fourth winter mode, this fourth spring mode obtained from the PCA shows also a col (Bluestein, 1992). With this configuration, severe winds blow over most of Europe (Figure III-6). Finally, the fifth mode presents a spatial pattern very similar to an omega blocking situation (Bluestein, 1992). In the region of the block, the weather remains essentially unchanged, as any transient weather disturbances are forced to circumvent the block (Figure III-6).

3.3. Meteorological analysis of the first modes in winter. Regional variable

The following descriptions are the PCA results of the winter daily wind data in the selected period described in the previous chapter. Prior to the spatial statistical results, the table with the explained variance percentages for the most significant PCs or modes for the wind speed field is shown. Subsequently, the eigenvectors with the associated meteorological descriptions are explained.

Componente	PCP(var)
1	37.85
2	11.47
3	7.21
4	4.77
5	4.45
6	3.60
7	2.87
8	2.75
9	2.49
10	2.35

Table 3.2. Variance percentages of the first ten PCs for the winter wind speed field.

Concerning wind regime, Iberia is characterized by a maximum in spring, minimum strength in summer and high frequency of calm in winter, exhibiting important climatic contrasts. The northern Peninsular area is mainly affected by cold dry or moist wind, depending on the air mass origin, while the south of Iberia is affected by southwestern warm dry winds coming from North Africa or by warm wet air masses coming from the southeast. To quote some winds as an example (see Figure III-9), the Mediterranean Peninsular coast is affected by wet winds named Levante or by wet and warm air masses coming from Sahara, the Xaloc. The northwestern (southeastern) cold (warm) dry (moist) winds blowing down (up)-valley Ebro are known as Cierzo (Bochorno) while west-northwestern moist cold winds, named Galema blow the Cantabric coasts (Font, 2000; García, 1985). On the other hand, Tramontana are northern or northeastern winds affecting Catalonia and the Balearics. Southern Iberia is influenced by winds such as Ábrego with different characteristics to those of the northern Peninsula. Therefore, there are significant northern-southern differences, advection of west-east air mass with diverse characteristics, influence of orography and land-sea temperature contrasts. Extreme wind events have disastrous consequences which can affect natural ecosystems and several aspects of societies. Therefore, advances in understanding the relationships of wind anomalies in the Iberian Peninsula with coherent atmospheric anomaly patterns constitute an issue of relevance.

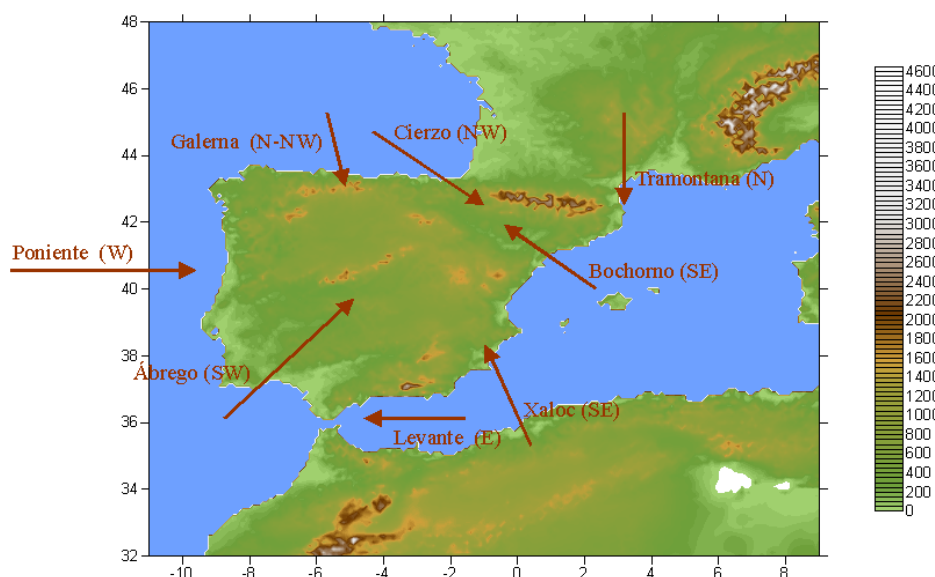


Figure III-9. The Iberian Peninsula with typical winds and directions superimposed

In the Figure III-10 and Figure III-11, eigenvectors or spatial patterns and their corresponding time series of the first ten modes obtained from the PCA applied to the regional variable are shown. The wind speed correlation isolines can be observed in the Figure III-10, highlighting areas of different wind behaviour over Iberia. Thus, in the first PC it is underlined the area corresponding to the North Iberian Plateau, displaying high correlation values covering the León, Salamanca and Valladolid area (see Figure II-4). The second PC shows a west-east isoline distribution, highlighting the Catalonia area. This zone is characterized by strong Tramontana. As it is abovementioned, the Tramontana are northern or northeastern winds affecting Catalonia and the Balearics. The third PC of Figure III-10 shows a north-south isoline configuration, depicting high correlation values around the Gibraltar Strait. Same behaviour is noted around the Gibraltar area in the PC5. PC4 and PC9 present similar configuration with isolines marking two different zones, the northeast and the southwest areas flanking an area that cover the two Plateaus.

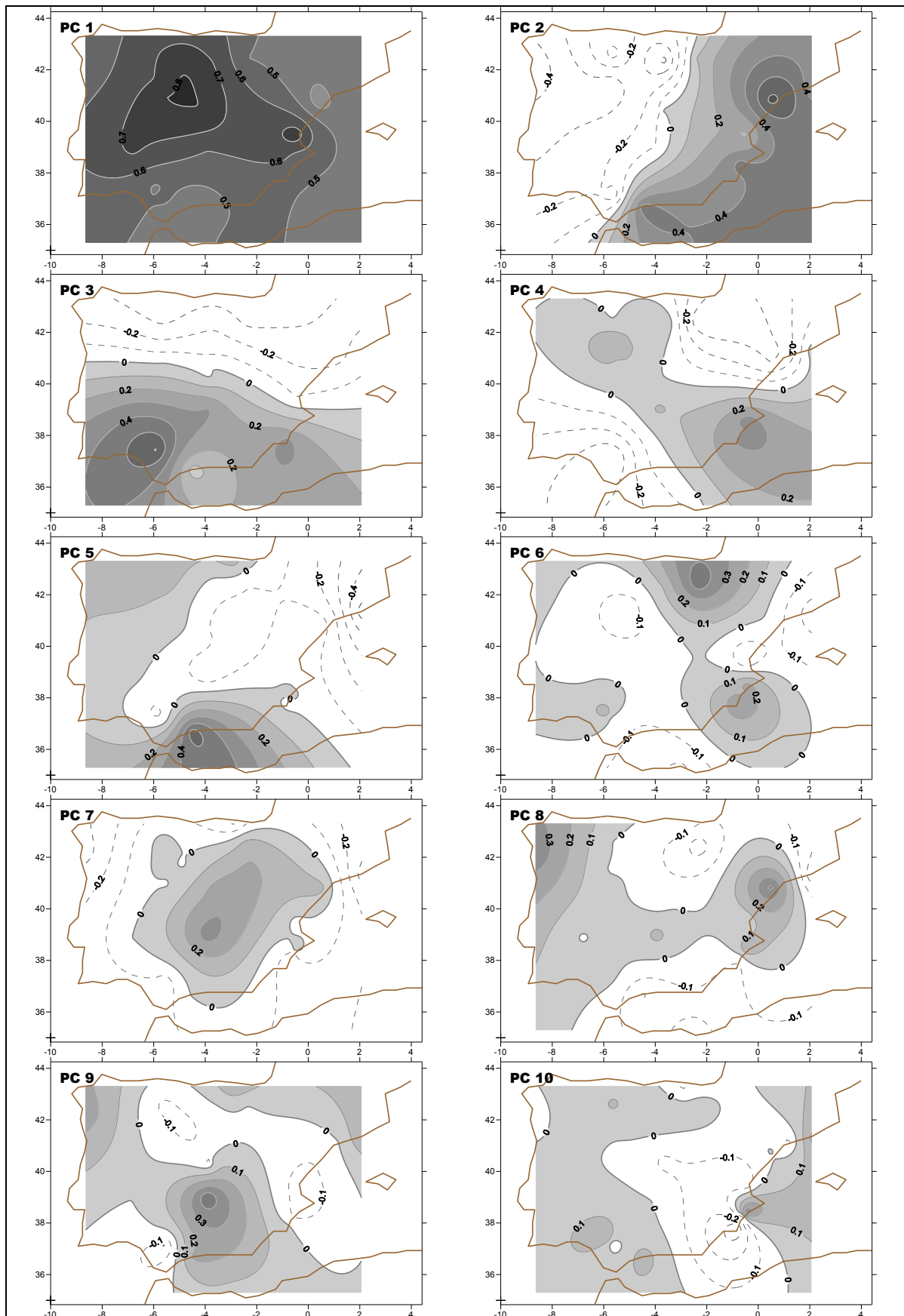


Figure III-10. The first ten PCA patterns of wind speed for winter. Contours indicate correlation values.

PC6 and PC8 suggest some similar information about the wind speed behaviour. The Ebro Valley channelling is highlighted with high (low) correlation values in the PC6 (PC8) while the Valencia area is underlined by low (high) correlation ones in the PC6 (PC8). The remainder PCs of Figure III-10, the seventh and the tenth ones, emphasize the wind speed behaviour over the South Iberian Plateau, giving different and weaker correlation values in the rest of the Iberian Peninsula.

Figure III-11 shows the evolution of the first ten PC time series of the wind speed over Iberia. Each panel highlights some characteristics associated to the wind behaviour. For sake of brevity, in this study the wavelet spectrum of the first time series has been shown. The first spatial pattern in Figure III-10 showed a similar wind behaviour over Iberia, underlying areas corresponding to the North Iberian Plateau. This behaviour is also represented in the corresponding time series of Figure III-11 with predominantly positive score values throughout the selected period (1970-2001).

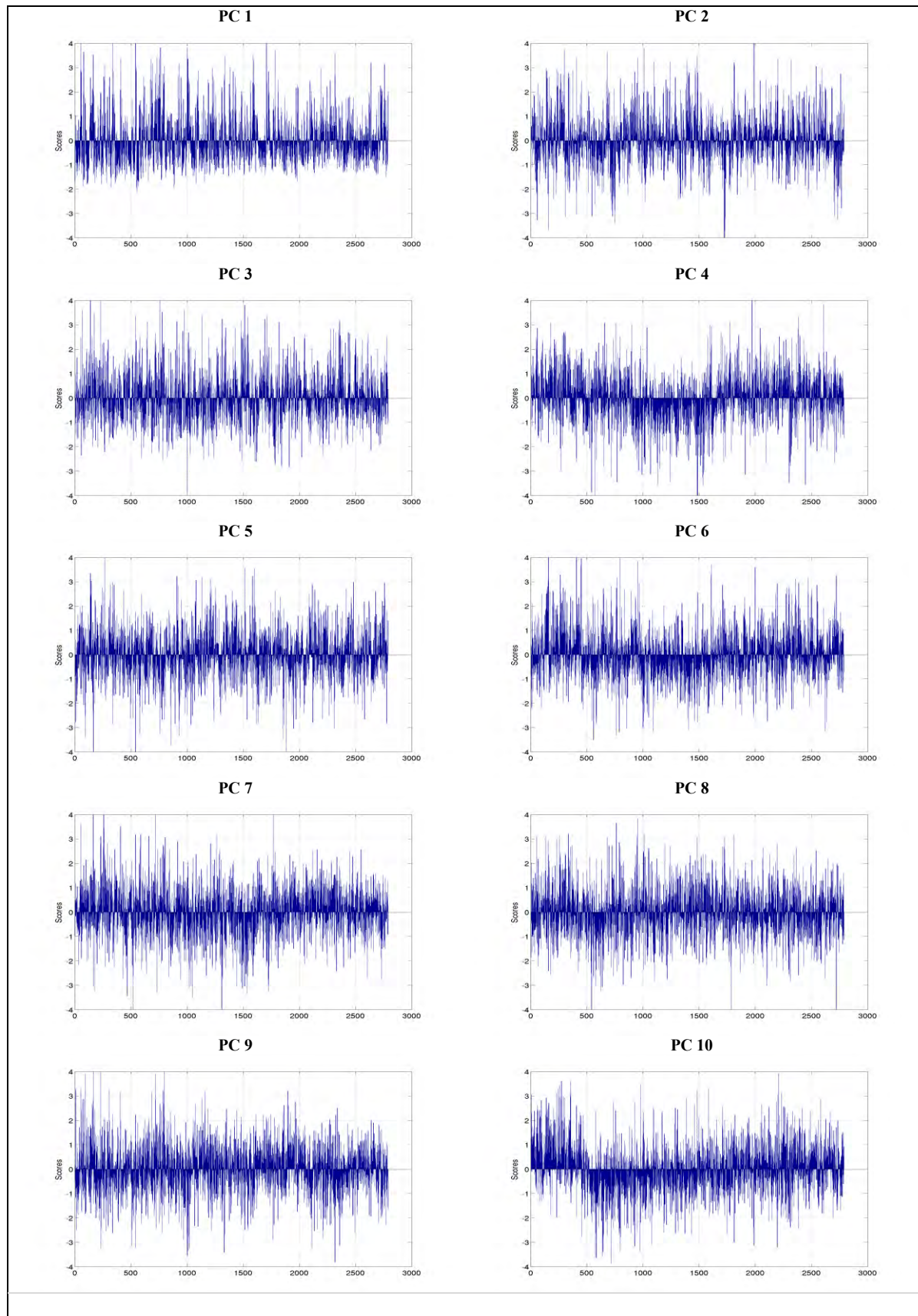


Figure III-11: Time series of PCs corresponding with the first ten modes of wind speed for winter.

In the spectrum wavelet, the power spectrum intensity (Figure III-12) is mainly concentrated in periods between 3 and 8 years, with highly energetic amplitude centred around 1976 and 1982, being noticeable a maximum absolute nucleus on 1980 and 1984 with a period with maximum amplitude around 6 years.

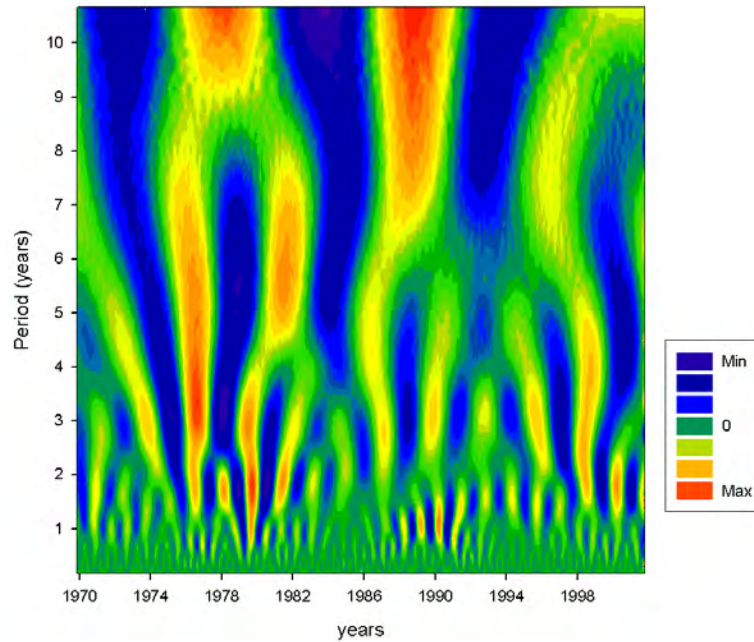


Figure III-12: The wavelet power spectrum of the wind speed time series corresponding to the first PC. The y-axis represents the variability scale (years) and the x-axis corresponds to the time period.

Moreover, throughout the record, some episodes of quasi-biennial oscillation (QBO) are found in Figure III-12, lasting a short time. QBO signal predominates during the period 1974-1982, exhibiting high intensity around 1980.

3.4. Meteorological analysis of the first modes in spring. Regional variable

In this section, the PCA results of the spring daily wind data in the selected period are described. For sake of brevity, the first five PCs are shown. These five modes account for more than 60 % of the total variance of the original data.

In the Figure III-13 and Figure III-14, eigenvectors and their corresponding time series of these first five modes, obtained from the PCA applied to the regional variable in springtime, are shown. Spring wind behaviour is very similar to the winter one. Thus, the first PC it is underlined the area corresponding to the North Iberian Plateau, displaying high correlation values covering the León, Salamanca and Valladolid area. The second PC shows a west-east isoline distribution, highlighting the northwestern Iberian area. The third PC of Figure III-13 shows a north-south isoline configuration, depicting high correlation values around the Catalonia area, which is associated to Tramontana. PC4 and PC5 present a configuration with isolines marking two different zones over Iberia, Plateaus and Gibraltar Strait.

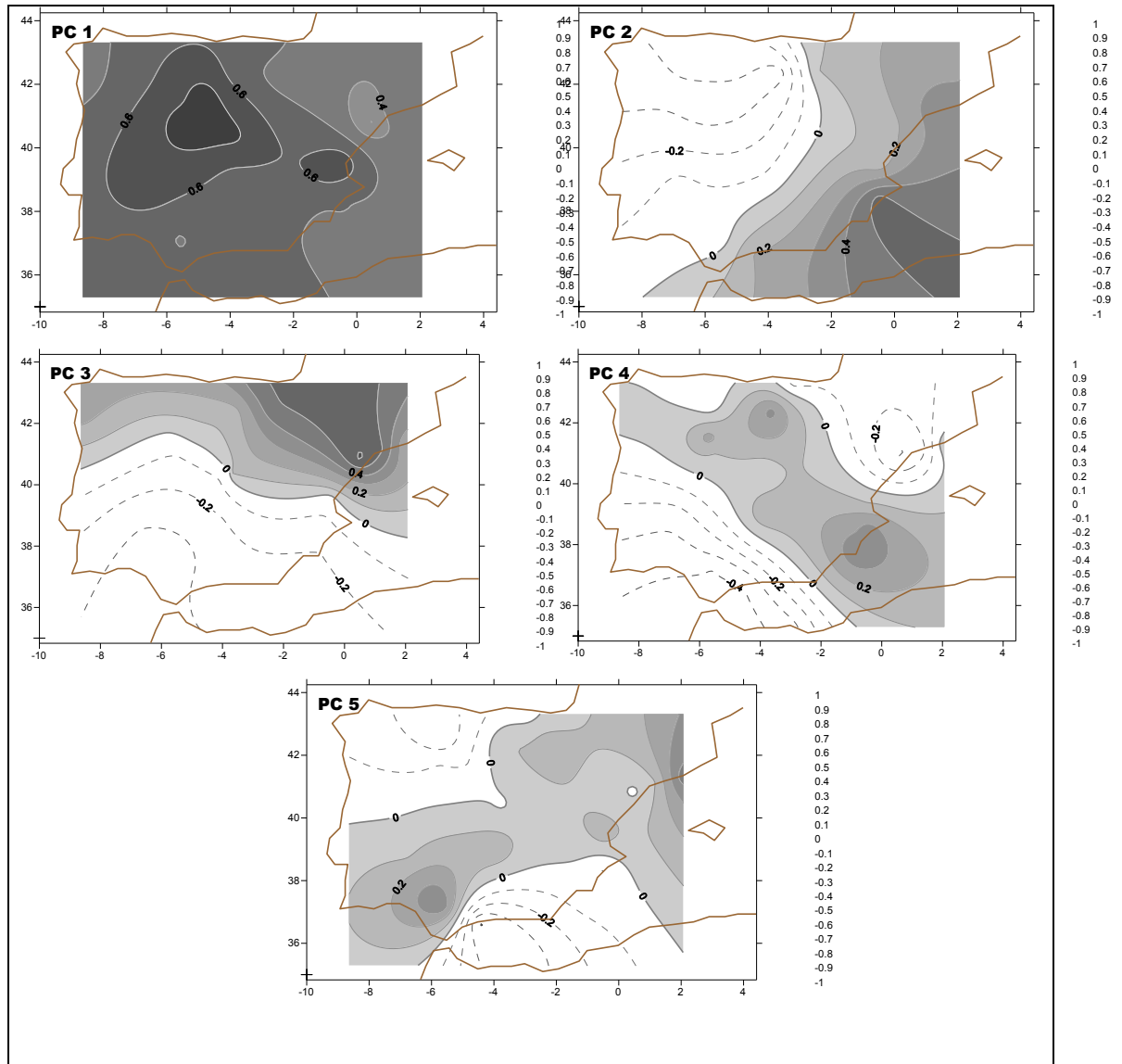


Figure III-13. The first five PCA patterns of wind speed for spring. Contours indicate correlation values.

Figure III-14 shows the evolution of the first five PC time series of the wind speed over Iberia. Same as in the winter case, each panel emphasizes characteristics related to the wind behaviour. The similar wind behaviour over Iberia is remarkable in the first spatial pattern (Figure III-13), showing areas with high positive correlations over the whole Iberia and especially in the North Iberian Plateau. This behaviour is also reproduced in the corresponding time series of Figure III-14 with predominantly positive score values throughout the selected period (1970-2001).

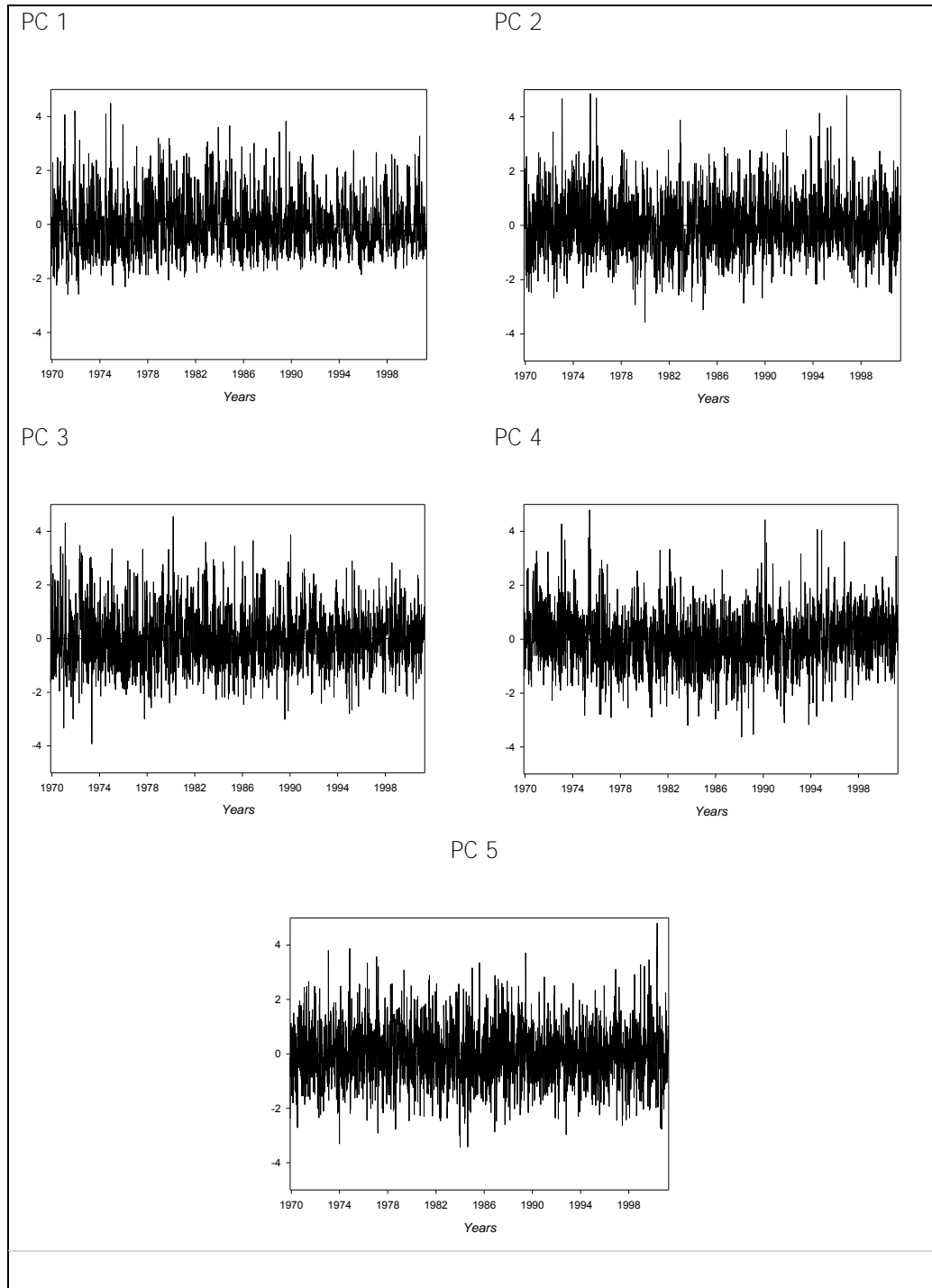


Figure III-14: Time series of PCs corresponding with the first five modes of wind speed for spring.

The power spectrum intensity of the first PC time series (Figure III-15) is mainly concentrated in periods corresponding to the low-frequency, i.e., periods greater than 3 years. In particular, it is remarkable highly energetic amplitude centred on 1980 and 1996, with a period with maximum amplitude around 5 years.

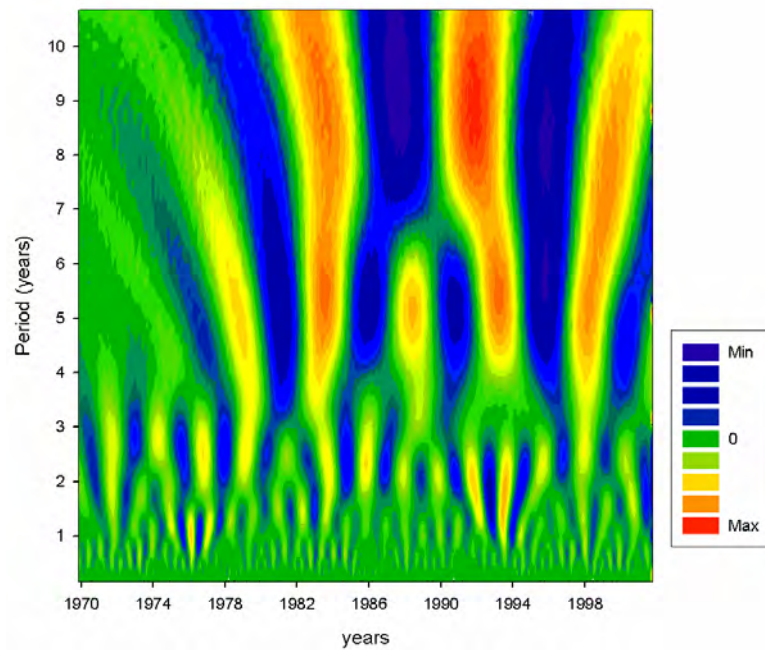


Figure III-15: The wavelet power spectrum of the wind speed time series corresponding to the first PC. The y-axis represents the variability scale (years) and the x-axis corresponds to the time period.

Throughout the record, some episodes of quasi-biennial oscillation (QBO) are also found (Figure III-15), exhibiting high intensity around 1992.

